

Short communication

## Use of in situ polymerized phenol-formaldehyde resin to modify a Nafion<sup>®</sup> membrane for the direct methanol fuel cell

Zhimou Wu<sup>a,b</sup>, Gongquan Sun<sup>a,\*</sup>, Wei Jin<sup>a,b</sup>, Qi Wang<sup>a,b</sup>, Hongying Hou<sup>a,b</sup>,  
Kwong-Yu Chan<sup>c</sup>, Qin Xin<sup>a,d</sup>

<sup>a</sup> Direct Alcohol Fuel Cells Laboratory, Dalian Institute of Chemical Physics, Chinese Academy of Sciences, Dalian 116023, China

<sup>b</sup> Graduate School of the Chinese Academy Sciences, Beijing 100039, China

<sup>c</sup> Department of Chemistry, The University of Hong Kong, Pokfulam Road, Hong Kong SAR, China

<sup>d</sup> State Key Laboratory of Catalysis, Dalian Institute of Chemical Physics, Chinese Academy of Sciences, Dalian 116023, China

Received 31 December 2006; received in revised form 7 February 2007; accepted 8 February 2007

Available online 25 February 2007

### Abstract

Commercial Nafion<sup>®</sup>-115 (trademark registered to DuPont) membranes were modified by in situ polymerized phenol formaldehyde resin (PFR) to suppress methanol crossover, and SO<sub>3</sub><sup>-</sup> groups were introduced to PFR by post-sulfonation. A series of membranes with different sulfonated phenol formaldehyde resin (sPFR) loadings have been fabricated and investigated. SEM-EDX characterization shows that the PFR was well dispersed throughout the Nafion<sup>®</sup> membrane. The composite membranes have a similar or slightly lower proton conductivity compared with a native Nafion<sup>®</sup> membrane, but show a significant reduction in methanol crossover (the methanol permeability of sPFR/Nafion<sup>®</sup> composite membrane with 2.3 wt.% sPFR loading was  $1.5 \times 10^{-6} \text{ cm}^2 \text{ s}^{-1}$ , compared with the  $2.5 \times 10^{-6} \text{ cm}^2 \text{ s}^{-1}$  for the native Nafion<sup>®</sup> membrane). In direct methanol fuel cell (DMFC) evaluation, the membrane electrode assembly (MEA) using a composite membrane with a 2.3 wt.% sPFR loading shows a higher performance than that of a native Nafion<sup>®</sup> membrane with 1 M methanol feed, and at higher methanol concentrations (5 M), the composite membrane achieved a 114 mW cm<sup>-2</sup> maximum power density, while the maximum power density of the native Nafion<sup>®</sup> was only 78 mW cm<sup>-2</sup>. © 2007 Elsevier B.V. All rights reserved.

**Keywords:** Direct methanol fuel cell; Methanol crossover; Nafion<sup>®</sup>; Phenol-formaldehyde resin; Composite membrane

### 1. Introduction

In recent years, there has been considerable interest in the development of direct methanol fuel cells. Methanol is an attractive fuel because its high energy density compare with hydrogen, and it is a low cost liquid that is easy to handle, store and transport [1,2]. DMFC could be the potential power source of several applications including portable electronics, distributed energy, and transportation [3,4]. There are two main barriers to the utilization of the DMFC. One is methanol crossover across the polymer electrolyte membrane from the anode to the cathode, which will affect the cell performance and lower the fuel efficiency [5,6]. The other is the poor methanol electro-oxidation kinetics of the anode [7].

Typically a perfluorofulfonic acid, such as a Nafion<sup>®</sup> membrane is used in DMFCs, due to good mechanical properties, chemical stability and high proton conductivity [8]. However, these membranes show a high methanol permeability [5,9]. Therefore, intensive interest has arisen in modifying membranes based on Nafion<sup>®</sup>.

In the recent past, more research groups have turned their attentions to developing composite membranes based on Nafion<sup>®</sup> to suppress the methanol crossover by using a variety of materials. One of the approaches is the solution casting of a mixed Nafion<sup>®</sup> solution with silica [10–12], silica doped with heteropolyacids [13], montmorillonite [14], titania [15], zeolite [16], zirconia, alumina [17], and vinylidene fluoride hexafluoropropylene copolymer [18]. The other approach is the impregnation of commercial Nafion<sup>®</sup> membrane with materials, such as silicon oxide [19–21], Pd [22], zirconium phosphates [23], polypyrrole [24,25], and polyfurfuryl alcohol [26]. There is phase separation occurring in a Nafion<sup>®</sup> polymer:

\* Corresponding author. Tel.: +86 411 84379063; fax: +86 411 84379063.  
E-mail address: [gqsun@dicp.ac.cn](mailto:gqsun@dicp.ac.cn) (G. Sun).

a hydrophobic backbone fluorocarbon phase, a hydrophilic region with the side-chains, and fixed  $\text{SO}_3^-$  end groups form adjacent aqueous domains for the liquid transportation channel and proton conductivity [27,28]. For the impregnation method, the hydrophilic regions provide the reaction cage for the fillers. Thus, the fillers will block the methanol transport channel and increase the zigzag of the channel. These composite membranes can more or less reduce methanol crossover, but at the same time decrease the proton conductivity, which will lower the cell performance.

In this work, we fabricated sPFR/Nafion<sup>®</sup> composite membranes by the impregnation-reaction method. First phenol-formaldehyde in solution impregnated Nafion<sup>®</sup> hydrophilic region, then in situ polymerization took place in the structure by acid catalysis of the solid acid-Nafion<sup>®</sup> under evaluated temperature. Finally, the functional group of the PFR in the membrane was sulfonated by concentrated sulfuric acid. These membranes showed a similar proton conductivity to Nafion<sup>®</sup>, but significantly suppressed methanol crossover. These characteristics suggest the potential application of a sPFR/Nafion<sup>®</sup> composite membrane in DMFCs at high methanol concentrations.

## 2. Experimental

### 2.1. Membrane preparation

Commercial Nafion<sup>®</sup>-115 membranes were cut into 4.0 cm × 4.0 cm pieces. The membranes were treated in boiling hydrogen peroxide (3 wt.%) for 2 h, followed by rinsing with deionized water, then protonized by treating them in boiling 0.5 M sulfuric acid for 2 h followed by washing with deionized water several times to remove the excess acid. The treated membranes were then stored in deionized water for later use. The membranes were dried in 120 °C oven for 24 h, and immersed in a solution of 6.0 g phenol, 5.3 g formaldehyde (36%), 35.6 g 2-propanol and 32.2 g deionized water at room temperature. The reaction was carried out under acid catalysis of the sulfonic groups of Nafion<sup>®</sup> for 24 h. Subsequently, the membranes were placed in 120 °C oven for 24 h for further polymerization of phenol formaldehyde inside the Nafion<sup>®</sup> membrane. Then the membranes were put into 100 °C sulfuric acid (98%) for 2 h, using this process to sulfonate the PFR inside membrane and remove the PFR stuck to the Nafion<sup>®</sup> membrane surface. Finally, the membranes were boiled in 0.5 M sulfuric acid for 2 h, washed with deionized water, and dried in 120 °C oven for 24 h. sPFR/Nafion<sup>®</sup> composite membranes with different loadings of sPFR were obtained by repeating this procedure.

### 2.2. Fouriertransform infrared spectroscopy (FTIR)

The FTIR spectra were collected on a Nicolet Avatar-370 equipped with a DTGS detector and a ZnSe crystal (45° angle) as attenuated total reflection accessory (ATR). The pressure was equal in all ATR measurements to avoid the difference brought by the pressure and penetrating depth.

### 2.3. Scanning electron microscopy (SEM) investigations and energy dispersive X-ray (EDX) analysis

JEOL JSM-5600LV is used for membrane morphology investigation. Fluorine element distribution in membrane cross section was determined by Oxford Instruments X-ray Microanalysis 1350.

### 2.4. Proton conductivity

The proton conductivity of membrane was obtained using ac impedance spectroscopy with potentiostat (EG&G Model 273A) and Lock-in amplifier (EG&G Model 5210) at room temperature (20 °C) and full humidity. The impedance was measured in the frequency range between 100 KHz and 1 Hz with a perturbation voltage amplitude of 10 mV. The proton conductivity  $\sigma$  was calculated from the impedance data, using the relation  $\sigma = L/RS$ , where  $L$  and  $S$  are the thickness and area of the membrane, respectively, and  $R$  was derived from the low intersect of the high frequency semicircle on a complex impedance plane with the  $\text{Re}(z)$  axis.

### 2.5. Methanol permeability

The methanol crossover through the membrane was measured by an open circuit potential method described in literatures [29,30]. The measurement performed on CHI 760B potentiostat/galvanostat at room temperature (20 °C). The membrane was clamped between two reservoirs of the diffusion cell (Fig. 1). Pt foil was used as a counter electrode (CE), and Ag/AgCl, KCl (saturated) was used as the reference electrode (RE). The gas diffusion electrode (GDE) was prepared by using carbon cloth (E-TEK) as substrates, and the Pt/C catalyst mixed with Nafion<sup>®</sup> was pasted on it. The Pt loading of GDE was 2 mg cm<sup>-2</sup>. Eq. (1) shows the relationship between the methanol concentration in compartment B and permeation time. Methanol permeability,  $P$  was calculated from Eq. (4)

$$J = V_B \frac{dC_{B(t)}}{dt} \frac{1}{S} = DK \frac{\Delta C}{L} \quad (1)$$

$$C_A \gg C_{B(t)}, \quad V_A \gg V_B \quad (2)$$

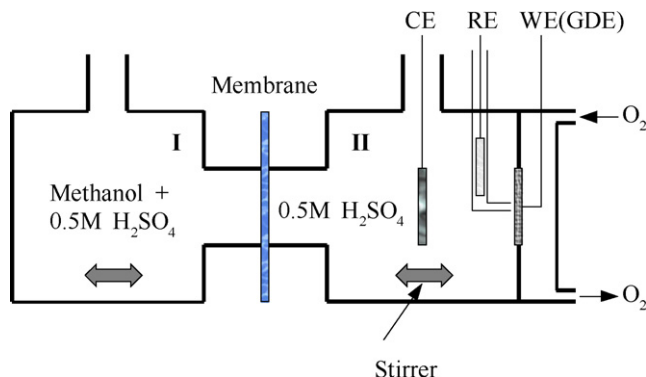


Fig. 1. Schematic diagram of diffusion cell for open circuit potential measurement.

$$\Delta C = C_A - C_B \approx C_{A(0)} \quad (3)$$

$$P = D \times K = \frac{V_B L}{S C_{A(0)}} \frac{\Delta C_{B(t)}}{\Delta t} \quad (4)$$

where  $J$  is the methanol flux in compartment B,  $V_A$  and  $V_B$  are the volume of compartments A and B, respectively,  $C_A$  and  $C_B$  are the methanol concentration of compartments A and B, respectively,  $D$  the diffusion coefficient,  $K$  the partition coefficient between the membrane and the adjacent solution,  $t$  the permeation time,  $S$  the effective area of membrane and  $L$  is the thickness of membrane.

### 2.6. DMFC single cell performance

The gas diffusion electrodes (GDEs) were prepared by hand brushing ink containing Nafion<sup>®</sup> dispersion and catalyst onto carbon paper diffusion substrates. Loadings of Pt–Ru/C (40%, Pt:Ru = 1:1, Johnson Matthey) at anode and Pt/C (40%, Johnson Matthey) at cathode were 2 and 1 mg cm<sup>-2</sup>, respectively. The MEA was prepared by sandwiching the membrane between the GDEs and then hot-pressed at 120 °C for 5 min at a pressure of 1.2 MPa. MEAs were tested in a single cell with 4 cm<sup>2</sup> flow channel area. The single cell was activated by 1 M methanol with 1 mL min<sup>-1</sup> feed at 75 °C without oxygen flow in cathode for 12 h. Then the cell was discharged several times at 75 °C with 1 mL min<sup>-1</sup> methanol flow rate, and oxygen at 0.2 MPa, flow rate 0.2 L min<sup>-1</sup>. After the cell remained stable, the single cell evaluation was operated at the same conditions.

## 3. Result and discussion

### 3.1. FTIR spectrum

Fig. 2 shows the FTIR spectra of Nafion<sup>®</sup>-115 and sPFR/Nafion<sup>®</sup> composite membrane. The two membranes all show the typical spectra of Nafion<sup>®</sup>. whereas the symmetric –SO<sub>3</sub><sup>-</sup> stretching band is clearly visible at about 1060 cm<sup>-1</sup>, this

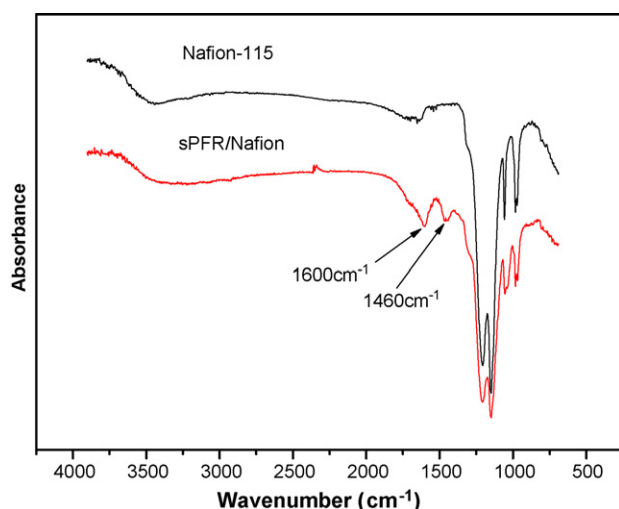


Fig. 2. FTIR spectra of Nafion<sup>®</sup>-115 native and sPFR/Nafion<sup>®</sup> composite membrane.

$\nu(\text{SO}_3^-)$  band will shift up or down depending on the hydration condition. The peaks at 1208, 1148, 1054, 982 and 968 cm<sup>-1</sup> are ascribed to characteristic functional groups in Nafion<sup>®</sup> [31]. The new distinct bands at 1600, 1460 cm<sup>-1</sup> are attributed to the characteristic vibrations of the benzene group.

### 3.2. SEM micrograph and EDX analysis

The membranes were freeze-fractured in liquid nitrogen, and the fracture surfaces were sputter coated with gold prior to scanning. Fig. 3 shows the SEM images of the membranes cross-section and their corresponding EDX mappings for fluorine atoms. In the EDX mapping image, the bright dots highlighted the high element concentration areas. Obviously, a homogeneous distribution of the fluorine element was observed in both two EDX mapping images which implied the PFR was well dispersed throughout the Nafion<sup>®</sup> membrane. The EDX mapping of native Nafion<sup>®</sup> (Fig. 3(c)) showed a much higher fluorine element concentration than that of sPFR/Nafion<sup>®</sup> composite membrane (Fig. 3(d)) despite the composite membrane had a higher thickness, which indicated some polymer chains of Nafion<sup>®</sup> had been embedded in PFR, which decreased the fluorine signal.

### 3.3. Proton conductivity

Table 1 shows the proton conductivity of native Nafion<sup>®</sup> membrane and sPFR/Nafion<sup>®</sup> composite membranes. Obviously, composite membranes achieved the similar or slightly lower proton conductivity of native Nafion<sup>®</sup> membrane. Although the integrated sPFR inside Nafion<sup>®</sup> membrane will block the proton transport channel, the dimension expansion (for example, the dimension of 8.9 wt.% sPFR loading membrane is 5.0 cm × 3.9 cm × 173 μm compared with 4.0 cm × 4.0 cm × 150 μm of native Nafion<sup>®</sup>-115 membrane) of composite membrane will some more decrease this block; on the other hand, the SO<sub>3</sub><sup>-</sup> group formed adjacent aqueous domains of sulfonated sPFR will provide additional proton transport capacity.

### 3.4. Methanol permeability

The methanol permeability was measured by open circuit potential method at ambient temperature. Fig. 4 shows the

Table 1  
Proton conductivity at room temperature of native Nafion<sup>®</sup>-115 membrane and sPFR/Nafion<sup>®</sup> composite membranes with different sPFR loadings

sPFR content (wt.%)	Proton conductivity (S/cm, × 10 <sup>-2</sup> )
0	3.6
0.3	2.7
1.7	3.6
2.3	3.1
3.9	2.9
6.2	3.5
8.9	3.1

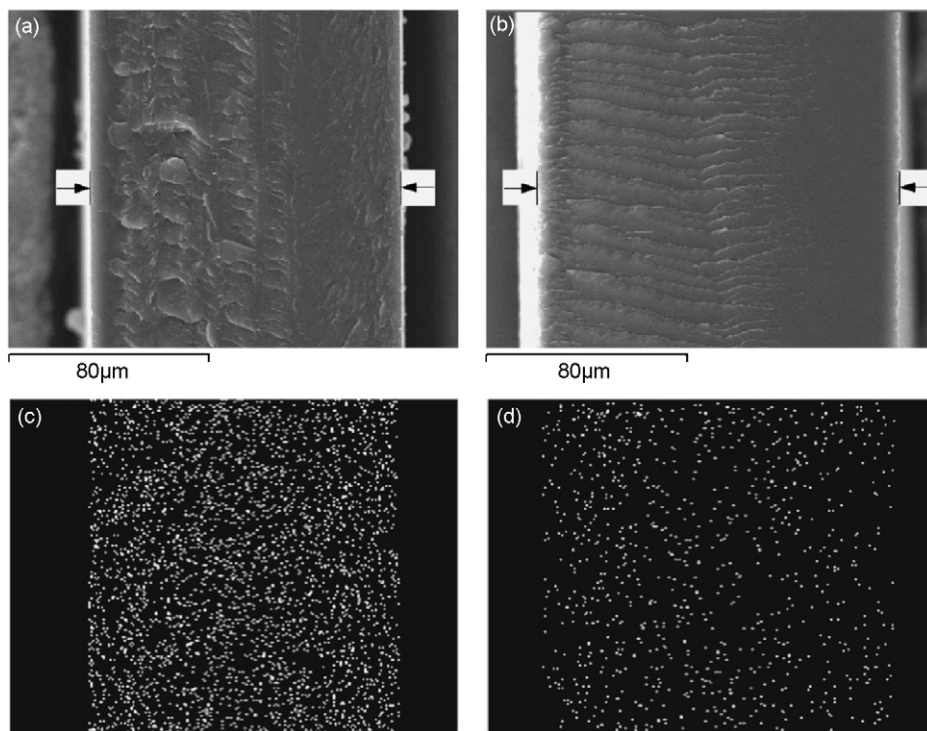


Fig. 3. SEM image and fluorine element EDX mapping image of the native Nafion<sup>®</sup> membrane and the 2.3 wt.% sPFR/Nafion<sup>®</sup> membrane cross-section: (a) SEM image of native Nafion<sup>®</sup> membrane; (b) SEM image of 2.3 wt.% sPFR/Nafion<sup>®</sup> membrane; (c) EDX mapping for the element F of native Nafion<sup>®</sup> membrane; (d) EDX mapping for the element F of 2.3 wt.% sPFR/Nafion<sup>®</sup> membrane.

working curve. The potential drop can be described by Nernst equation [29]. The concentration of methanol in compartment B will increase with the permeating time elapse during test. This methanol permeating from compartments A to B will cause the GDE potential dropping continually. Thus, the methanol concentration in compartment B can be determined by this drop from the working curve. From Eq. (4),  $\Delta C_{B(t)}/\Delta t$  will be near a constant after the  $V_A$ ,  $V_B$ ,  $S$ ,  $C_{A(0)}$  and  $d$  were fixed and the  $P$  value is lower enough. The sPFR/Nafion<sup>®</sup> composite membrane with 3.9 wt.% sPFR loading was chose for demonstrating this process. Fig. 5 shows the GDE potential dropping and methanol concen-

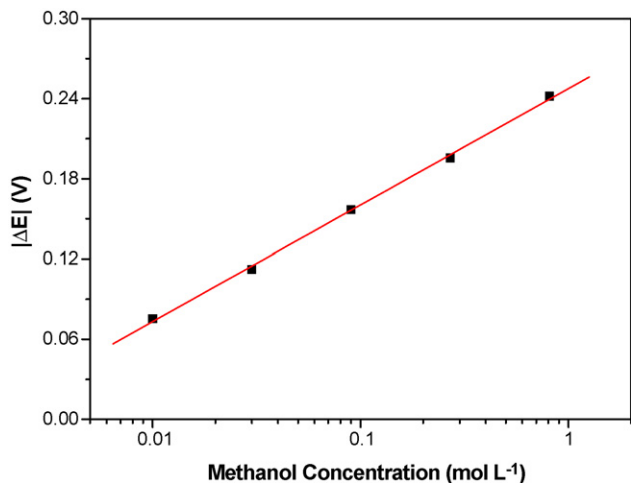


Fig. 4. Potential drop  $|\Delta E|$  against methanol concentration.

tration in compartment B increasing with the permeation time elapse (compartment A was filled with 5 M methanol and 0.5 M H<sub>2</sub>SO<sub>4</sub>, while compartment B was filled with 0.5 M H<sub>2</sub>SO<sub>4</sub>). Apparently, the crossover methanol concentration is increasing linearly with the permeation time elapse. The  $\Delta C_{B(t)}/\Delta t$  value can be got from the slope of the methanol concentration–time curve. Fig. 6 compares the methanol permeability and thickness of composite membrane with different sPFR loadings. It can be seen only few sPFR incorporated in Nafion<sup>®</sup> membrane will significantly suppress the methanol crossover. The methanol permeability of sPFR/Nafion<sup>®</sup> composite membrane with 2.3 wt.% sPFR loading was  $1.5 \times 10^{-6} \text{ cm}^2 \text{ s}^{-1}$ , compared with the  $2.5 \times 10^{-6} \text{ cm}^2 \text{ s}^{-1}$  of the native Nafion<sup>®</sup> membrane. It

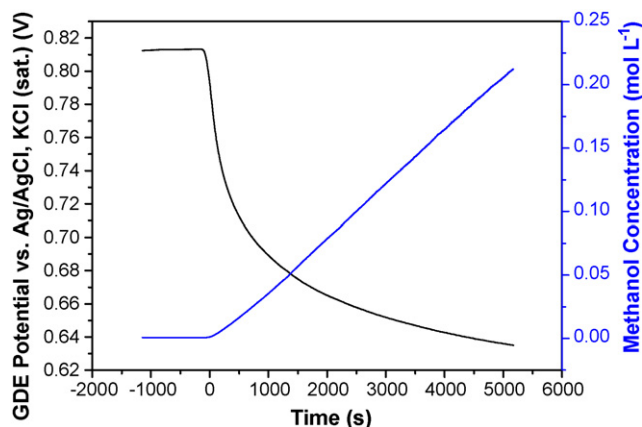


Fig. 5. GDE potential dropping and methanol concentration vs. permeation time (sPFR/Nafion<sup>®</sup> composite membrane with 3.9 wt.% sPFR).



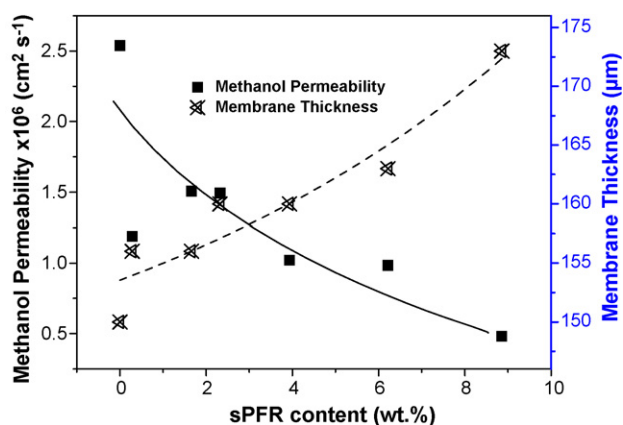


Fig. 6. Methanol permeability and thickness of composite membrane with different sPFR loadings.

is noted that the methanol permeability of Nafion<sup>®</sup> 115 agreed well with literature data [32]. And the methanol permeation of composite membrane decreased gradually with the sPFR loading increase. This indicated the sPFR was likely filled in hydrophilic region of Nafion<sup>®</sup> formed by the side chain  $\text{SO}_3^-$  end group adjacent aqueous domains, which provided the transport channel for the liquid. With increasing sPFR contents in Nafion<sup>®</sup> membrane, more and more “free space” inside swelling Nafion<sup>®</sup> membrane will be filled with sPFR, which caused the expansion of membrane, and the methanol transport channel will be further blocked. This is in agreement with the SEM–EDX analysis.

### 3.5. DMFC single cell performance

sPFR/Nafion<sup>®</sup> composite membrane with 2.3 wt.% loading was chosen for DMFC single cell performance evaluation, since this membrane had the lowest selectivity ( $\phi = \sigma/P$ ,  $2.1 \times 10^4 \text{ S s cm}^{-3}$ ) compared with other composite membrane, and that is higher than that of native Nafion<sup>®</sup> membrane ( $1.4 \times 10^4 \text{ S s cm}^{-3}$ ). Figs. 7 and 8 show the DMFC single cell performance with the native Nafion<sup>®</sup>-115 membrane and sPFR/Nafion<sup>®</sup> composite membrane using 1 and 5 M methanol at 75 °C, respectively. The composite membranes improved the

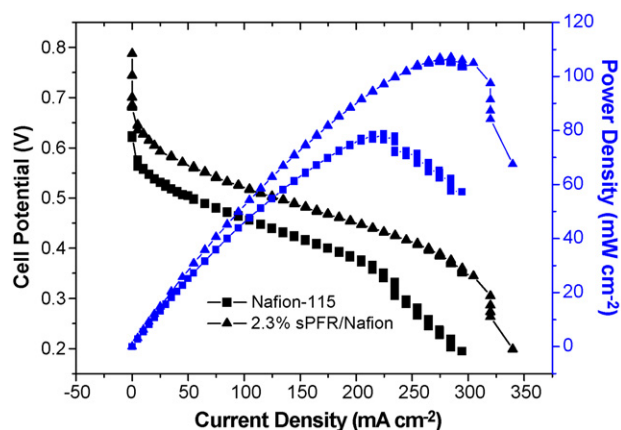


Fig. 7. Polarization curves of native Nafion<sup>®</sup>-115 membrane and sPFR/Nafion<sup>®</sup> membrane with 2.3 wt.% sPFR loading, 1 M methanol.

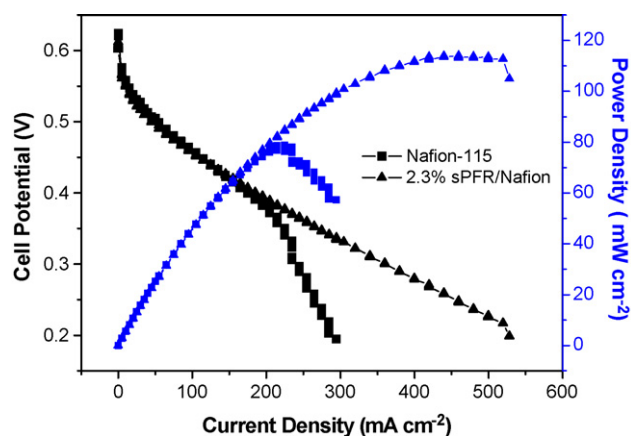


Fig. 8. Polarization curves of native Nafion<sup>®</sup>-115 membrane and 2.3% sPFR/Nafion<sup>®</sup> membrane, 5 M methanol.

performance at both methanol concentrations compared with the native Nafion<sup>®</sup> membrane. The composite membrane showed a higher performance than native Nafion<sup>®</sup> membrane with a 1 M methanol feed. This was attributed to lower methanol crossover of this composite membrane which raised the cell potential more than the reduced IR loss decreases the cell potential in comparison with native Nafion<sup>®</sup>. At higher methanol concentrations (5 M), the composite membrane achieved  $114 \text{ mW cm}^{-2}$  maximum power density, while the maximum power density of native Nafion<sup>®</sup> membrane was only  $78 \text{ mW cm}^{-2}$ . These results suggest the potential application of a sPFR/Nafion<sup>®</sup> composite membrane in DMFCs with high methanol concentrations.

## 4. Conclusion

Composite sPFR/Nafion<sup>®</sup> membranes were successfully prepared by in situ polymerization of phenol formaldehyde, and the PFR in the membrane was sulfonated by using  $\text{H}_2\text{SO}_4$  (98%) at 100 °C for 2 h. SEM–EDX characterization shows the PFR was well dispersed throughout the Nafion<sup>®</sup> membrane. Compared with a native Nafion<sup>®</sup> membrane, the sPFR/Nafion<sup>®</sup> membranes had a similar proton conductivity, but significantly decreased the methanol crossover. The methanol permeability of the sPFR/Nafion<sup>®</sup> composite membrane with 2.3 wt.% sPFR loading was  $1.5 \times 10^{-6} \text{ cm}^2 \text{ s}^{-1}$ , compared to  $2.5 \times 10^{-6} \text{ cm}^2 \text{ s}^{-1}$  for the native Nafion<sup>®</sup> membrane. Due to a much lower methanol crossover, the sPFR/Nafion<sup>®</sup> composite membrane with 2.3 wt.% sPFR loading showed a higher DMFC performance for 1 M methanol feed, and achieved a maximum power density of  $114 \text{ mW cm}^{-2}$  with a 5 M methanol feed, compared with the  $78 \text{ mW cm}^{-2}$  for native Nafion<sup>®</sup>. These results suggest the potential application of the sPFR/Nafion<sup>®</sup> membrane in DMFCs at high methanol concentrations.

## Acknowledgement

This work was financially supported by National Natural Science Foundation of China (Grant Nos. 50575036 and 50676093).

## References

- [1] B.D. McNicol, D.A.J. Rand, K.R. Williams, *J. Power Sources* 83 (1999) 15–31.
- [2] X. Ren, P. Zelenay, S. Thomas, J. Davey, S. Gottesfeld, *J. Power Sources* 86 (2000) 111–116.
- [3] A.S. Aricò, S. Srinivasan, V. Antonucci, *Fuel Cells* 1 (2001) 1–29.
- [4] R. Dillon, S. Srinivasa, A.S. Aricò, V. Antonucci, *J. Power Sources* 127 (2004) 112–126.
- [5] A. Heinzel, V.M. Barragán, *J. Power Sources* 84 (1999) 70–74.
- [6] H. Dohle, J. Divise, J. Mergel, H.F. Oetjen, C. Zingler, D. Stolten, *J. Power Sources* 105 (2002) 274–282.
- [7] C. Lamy, A. Lima, V. LeThum, F. Delime, C. Coutanceau, J.-M. Léger, *J. Power Sources* 105 (2002) 283–296.
- [8] D.E. Curtin, R.D. Lousenberg, T.J. Henry, P.C. Tangeman, M.E. Tisack, *J. Power Sources* 131 (2004) 41–48.
- [9] P.S. Kauranen, E. Skou, *J. Appl. Electrochem.* 26 (1996) 909–917.
- [10] H. Wang, B.A. Holmberg, L. Huang, Z. Wang, A. Mitra, J.M. Norbeck, Y. Yan, *J. Mater. Chem.* 12 (2002) 834–837.
- [11] C. Li, G. Sun, S. Ren, J. Liu, Q. Wang, Z. Wu, H. Sun, W. Jin, *J. Membr. Sci.* 272 (2006) 50–57.
- [12] R. Jiang, H.R. Kunz, J.M. Fenton, *J. Membr. Sci.* 272 (2006) 116–124.
- [13] H. Kim, Y. Shul, H. Han, *J. Power Sources* 158 (2006) 137–142.
- [14] C. Rhee, H. Kim, H. Chang, J. Lee, *Chem. Mater.* 17 (2005) 1691–1697.
- [15] V. Baglio, A.S. Aricò, A.D. Blasi, V. Antonucci, P.L. Antonucci, S. Licocchia, E. Traversa, F.S. Fiory, *Electrochim. Acta* 50 (2005) 1241–1246.
- [16] V. Tricoli, F. Nannetti, *Electrochim. Acta* 48 (2003) 2625–2633.
- [17] A.S. Aricò, V. Baglio, A.D. Blasi, P. Creti, P.L. Antonucci, V. Antonucci, *Solid State Ionics* 161 (2003) 251–265.
- [18] K. Cho, J. Eom, H. Jung, N. Choi, Y. Lee, J. Park, J. Choi, K. Park, Y. Sung, *Electrochim. Acta* 50 (2004) 583–588.
- [19] Q. Deng, R.B. Moore, K.A. Mauritz, *J. Appl. Polym. Sci.* 68 (1998) 747–763.
- [20] Y. Kim, W. Choi, S. Woo, W. Hong, *J. Membr. Sci.* 238 (2004) 213–222.
- [21] D.H. Junga, S.Y. Cho, D.H. Pecka, D.R. Shina, J.S. Kim, *J. Power Sources* 106 (2002) 173–177.
- [22] Y. Kim, K. Park, J. Choi, I. Park, Y. Sung, *Electrochem. Commun.* 5 (2003) 571–574.
- [23] F. Bauer, M. Willert-Porada, *J. Membr. Sci.* 233 (2004) 141–149.
- [24] A. Sungpet, *J. Membr. Sci.* 226 (2003) 131–134.
- [25] H.S. Park, Y.J. Kim, W.H. Hong, H.K. Lee, *J. Membr. Sci.* 272 (2006) 28–36.
- [26] J. Liu, H. Wang, S. Cheng, K.Y. Chan, *Chem. Commun.* 49 (2004) 728–729.
- [27] H.G. Haubold, T. Vad, H. Jungbluth, P. Hiller, *Electrochim. Acta* 46 (2001) 1559–1563.
- [28] K.A. Mauritz, R.B. Moore, *Chem. Rev.* 104 (2004) 4535–4585.
- [29] N. Munichandraiah, K. McGrath, G.K.S. Prakash, R. Aniszfeld, G.A. Olah, *J. Power Sources* 117 (2003) 98–101.
- [30] J. Liu, H. Wang, S. Cheng, K.Y. Chan, *J. Membr. Sci.* 246 (2005) 95–101.
- [31] M. Ludvigsson, J. Lindgren, J. Tegenfeldt, *Electrochim. Acta* 45 (2000) 2267–2271.
- [32] Z. Chen, B. Holmberg, W. Li, X. Wang, W. Deng, R. Munoz, Y. Yan, *Chem. Mater.* 18 (2006) 5669–5675.